# Iterative MAP algorithm for Gauss-Markov Channel

by

Ya-Ting Cho

Thesis submitted to the Institute of Communications Engineering
National Chiao Tung University, Taiwan
in partial fulfillment of the requirements
for the degree of Master of Science
2005

Advisory Committee:

Professor Po-Ning Chen, Advisor
Professor Yunghsiang S. Han
Professor Chung-Chin Lu
Professor Chung-Hsuan Wang

# ABSTRACT

In this paper, we experiment on the idea that the *channel-with-memory* nature can be nearly weakened to *blockwise independence* by the insertive transmission of informationless "random bits" (of length no less than the channel memory or channel spread) between two consecutive blocks. We found that these "random bits" can indeed be another parity check bits generated due to interleaved information bits such that additional coding information can be provided to improve the system performance. An examplified structure that follows this idea is the parallel concatenated convolutional code (PCCC). We thus derived its respective iterative MAP algorithm for time-varying channel with *first-order* Gauss-Markov fading, and tested whether or not the receiver can treat the received vector as blockwise independence with 2-bit blocks periodically separated by *single* parity-check bit from the second component recursive systematic convolutional (RSC) code encoder. Simulation results show that the iterative MAP decoder that is derived based on blockwise independence assumption not only performs close to the CSI(channel state information)-aided decoding scheme but is at most 0.9 dB away from the Shannon limit.

# ACKNOWLEDGMENTS

I owe my gratitude to all the people who have made this thesis possible and because of whom my graduate experience has been one that I will cherish forever.

TABLE OF CONTENTS

LIST OF FIGURES

# Chapter 1

# Introduction

## 1.1 Background

In recent years, the growing demand in wireless communications inspires a quick advance in wireless transmission technologies. These technologies blossom in both *high-mobility low-bit-rate* and *low-mobility high-bit-rate* transmissions. Apparently, the next challenge in wireless communications will be how to reach *high transmission rate* under *high mobility*.

The main technology obstacle for high-bit-rate transmission under high mobility is the seemingly highly time-varying channel characteristic due to movement; such a characteristic enforces the dependence between consecutive symbols, and further effects the difficulty in compensating the intersymbol interference. In principle, the temporal channel memory can be eliminated by an intersymbol space longer than the channel memory spread. An example is the IEEE 802.11a standard, in which 0.8-$\mu$s "intersymbol space" is added between two consecutive 3.2-$\mu$s OFDM symbols to combat any delay spread less than 800 nano seconds [5]. In order to take advantage of the circular convolution technique, the 0.8-$\mu$s "intersymbol space" is designed to be the leading 0.8-$\mu$ portion of the 3.2-$\mu$s OFDM symbol, which is often named the *cyclic prefix*.

In this work, we experiment on a different view in the neutralization of channel memory, where the "intersymbol space" may be of use to enhance the system performance. Specifically, we speculate that the received vector can be broken into *nearly time-independent* blocks by the insertive transmission of random bits of length no less than the channel memory. In order to make the best use of these interblock random bits, they can be designed to be the parity-check bits of the interleaved information bits, in which *interleaving* can provide the required randomness, and parity-check bits can provide additional coding information for further improvement of system performance. We then begin the experiment from the simplest case along this idea, i.e., the parallel concatenated convolutional code (PCCC) and its respective iterative MAP decoder over a time-varying channel with first-order Gauss-Markov fading [3, 4]. Simulation results hint that the iterative MAP decoder that is derived based on *blockwise independence* assumption not only performs close to the CSI(channel state information)-aided decoding scheme but is at most 0.9 dB away from the Shannon limit, thereby confirms the feasibility of our proposal. Details will be introduced in subsequent sections.

## 1.2 Outline of Thesis

This thesis is organized in the following fashion. In Chapter 2, we introduce the system model concerned in the paper. The metric functions used for the iterative MAP algorithm based on blockwise independence assumption are derived in Chapter 3. Chapter 4 devotes to the presentation and discussion of the simulation results. Final conclusion is given in Chapter 5.

# Chapter 2

# Gauss-Markov System Model

## 2.1 System model for Gauss-Markov fading

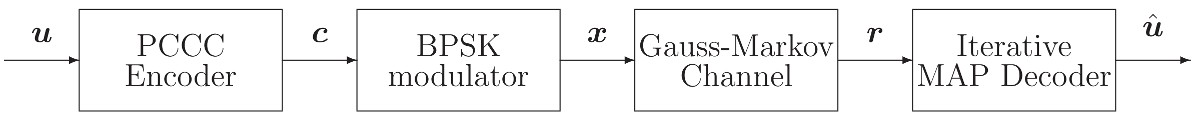


Figure 2.1: System model for coded transmission over Gauss-Markov channel.

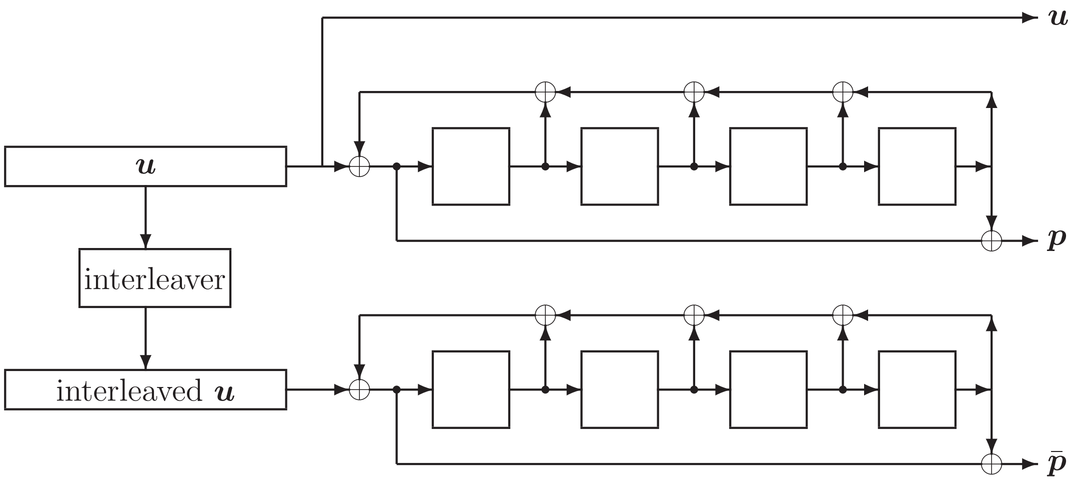


Figure 2.2: The PCCC encoder with $(37, 21)$ component RSC encoders.

Referring to Fig. 2.1, the information bit sequence $\boldsymbol{u} = [u_1, u_2, \cdots, u_K]$ is comprised of $K$ independent and identically distributed (i.i.d.) bits with equal probable marginal, where each $u_j$ is either 0 or 1. This information bit sequence is fed into a parallel concatenated convolutional code (PCCC) encoder that consists of two $(37, 21)$ recursive systematic convolutional (RSC) code encoders parallelly concatenated through an interleaver to generate the coded bit sequence

$$\boldsymbol{c} = [c_1, c_2, \cdots, c_N] = [u_1, p_1, \bar{p}_1, u_2, p_2, \bar{p}_2, \cdots, u_K, p_K, \bar{p}_K],$$

where $\boldsymbol{p} = [p_1, p_2, \cdots, p_K]$ and $\bar{\boldsymbol{p}} = [\bar{p}_1, \bar{p}_2, \cdots, \bar{p}_K]$ are respectively the parity bit sequences generated by the first and the second component RSC encoders (cf. Fig. 2.2). Antipodal modulation, i.e., $x_j = 2c_j - 1$, is then applied to the coded bit sequence before it is sent to the Gauss-Markov modelled time-varying channel. Finally, the received sequence $\boldsymbol{r} = [r_1, r_2, \cdots, r_N]$ is delivered to an iterative MAP decoder, and an estimate of the transmitted information bit sequence $\hat{\boldsymbol{u}} = [\hat{u}_1, \hat{u}_2, \cdots, \hat{u}_K]$ is outputted after sufficient number of iterations.

The channel model considered in this work is a complex-valued time-varying channel with Gauss-Markov fading; therefore, the received signal at time $j$ is given by:

$$r_j = h_j x_j + z_j, \tag{2.1}$$

where $[z_1, z_2, \cdots, z_N]$ is an i.i.d. complex-valued Gaussian-distributed noise sequence with zero marginal mean and marginal variance $E[z_j z_j^*] = \sigma^2$, and the channel coefficient $h_j$ is Gauss-Markov distributed, satisfying that $h_j = \alpha h_{j-1} + v_j$ for complex-valued scaling constant $\alpha$, complex-valued initial value $h_0$ and i.i.d. complex-valued Gaussian-distributed process $[v_1,\ v_2,\ \cdots,\ v_N]$ with $E[v_j] = 0$ and $E[v_j v_j^*] = \sigma_v^2$. The complex-valued constant $\alpha$ is a first-order Markov factor usually chosen according to $|\alpha| = e^{-\omega T}$, where $T$ is the system sampling period and $\omega/\pi$ is the Doppler spread [9]. Notably, although $x_j$ in our system is discrete real-valued (in fact, is either $+1$ or $-1$), the resultant $r_j$ is in general complex-valued due to its multiplication with complex $h_j$ and addition with complex $z_j$. Such a complex-valued system setting can mirror the practical effect of possible unsynchronization between the transmitter and the receiver, in addition to the phase delay due to channel fading.

Denote by $x_i^j$ the portion $[x_i, \cdots, x_j]$ of sequence $\boldsymbol{x}$. Similar notations are used for $r_i^j$ and $h_i^j$. Since the channel coefficient $h_i^j$ follows the Gauss-

Markov distribution,

$$f\left\{h_i^j\right\} = f\left\{h_i\right\} \prod_{k=i+1}^{j} f\left\{h_k|h_{k-1}\right\} = \frac{1}{\pi\bar{\sigma}_i^2} e^{-\frac{|h_i-\bar{h}_i|^2}{\bar{\sigma}_i^2}} \prod_{k=i+1}^{j} \frac{1}{\pi\sigma_v^2} e^{-\frac{|h_k-\alpha h_{k-1}|^2}{\sigma_v^2}},$$

where $\bar{h}_i = \alpha^i h_0$ and $\bar{\sigma}_i^2 = \sigma_v^2(1-|\alpha|^{2i})/(1-|\alpha|^2)$ are the mean and variance of Gaussian variable $h_i$, respectively. According to (2.1),

$$f\left\{r_i^j\left|h_i^j, x_i^j\right.\right\} = \prod_{k=i}^{j} f\left\{r_k|h_k, x_k\right\} = \prod_{k=i}^{j} \frac{1}{\pi\sigma^2} e^{-\frac{|r_k-x_k h_k|^2}{\sigma^2}}.$$

Therefore, it can be derived [3] that:

$$\begin{aligned}
& f\left\{r_i^j\left|x_i^j\right.\right\} \\
= & \int_{\mathcal{C}^{j-i+1}} f\left\{r_i^j, h_i^j\left|x_i^j\right.\right\} dh_i^j \\
= & \int_{\mathcal{C}^{j-i+1}} f\left\{r_i^j\left|x_i^j, h_i^j\right.\right\} f\left\{\left.h_i^j\right| x_i^j\right\} dh_i^j \\
= & \int_{\mathcal{C}^{j-i+1}} f\left\{r_i^j\left|x_i^j, h_i^j\right.\right\} f\left\{h_i^j\right\} dh_i^j \qquad (2.2)\\
= & \int_{\mathcal{C}^{j-i+1}} \left(\frac{1}{(\pi\sigma^2)^{j-i+1}} \prod_{k=i}^{j} e^{-\frac{|r_k-x_k h_k|^2}{\sigma^2}}\right) \\
& \qquad \left(\frac{1}{\pi^{j-i+1}\sigma_v^{2(j-i)}\bar{\sigma}_i^2} e^{-\frac{|h_i-\bar{h}_i|^2}{\bar{\sigma}_i^2}} \prod_{k=i+1}^{j} e^{-\frac{|h_k-\alpha h_{k-1}|^2}{\sigma_v^2}}\right) dh_i^j \\
= & \frac{e^{-\frac{|\bar{h}_i|^2}{\bar{\sigma}_i^2}}}{\pi^{j-i+1}\sigma^{2(j-i+1)}\sigma_v^{2(j-i)}\bar{\sigma}_i^2} \left(\prod_{k=i}^{j} e^{-|r_k|^2/\sigma^2} G_k e^{G_k|q_k|^2}\right), \qquad (2.3)
\end{aligned}$$

where $\mathcal{C} \triangleq \Re \times \Re$ is the entire domain for complex numbers, and (2.2) holds because $h_i^j$ is independent of $x_i^j$, and

$$G_k^{-1} \triangleq \begin{cases} \dfrac{1}{\sigma^2} + \dfrac{|\alpha|^2}{\sigma_v^2} + \dfrac{1}{\bar{\sigma}_k^2}, & \text{if } k = i; \\ \dfrac{1}{\sigma^2} + \dfrac{|\alpha|^2}{\sigma_v^2} + \dfrac{1}{\sigma_v^2} - \dfrac{|\alpha|^2 G_{k-1}}{\sigma_v^4}, & \text{if } i < k < j; \\ \dfrac{1}{\sigma^2} + \dfrac{1}{\sigma_v^2} - \dfrac{|\alpha|^2 G_{k-1}}{\sigma_v^4}, & \text{if } k = j, \end{cases}$$

and

$$q_k \triangleq \begin{cases} \dfrac{r_k x_k}{\sigma^2} + \dfrac{\bar{h}_k}{\bar{\sigma}_k^2}, & \text{if } k = i; \\ \dfrac{r_k x_k}{\sigma^2} + \dfrac{\alpha G_{k-1} q_{k-1}}{\sigma_v^2}, & \text{if } i < k \leq j, \end{cases}$$

By following similar derivation, we can generalize the MAP algorithm for Gauss-Markov fading channels in the next chapter.

# Chapter 3

# Iterative MAP Algorithm for Gauss-Markov Channel

## 3.1 Assumptions made for the metric derivation

In this chapter, we derive the metric functions, namely, $\alpha(\cdot)$, $\beta(\cdot)$ and $\gamma(\cdot)$, used by the iterative MAP decoder.

The metrics used in the first component decoder consider the effect of Gauss-Markov channel fading based on the assumption that the received scalers $r_{3i+1}^{3i+2}$ are *independent* of the previous received scalers $r_{3(i-1)+1}^{3(i-1)+2}$. It can be shown from simulations that a small bit-error-rate in information bit sequence $\boldsymbol{u}$ could induce up to half parity-check-bit errors because of the error-propagation nature of the component RSC encoder. This observation, together with the effect of interleaver, results in that the parity check bits $[x_3, x_6, x_9, \cdots]$ due to the *interleaved* $\boldsymbol{u}$ is almost *bit-wisely independent* of the *uninterleaved* $\boldsymbol{u} = [x_1, x_4, x_7, \cdots]$, as well as the parity check bit sequence $[x_2, x_5, x_8, \cdots]$ generated according to the *uninterleaved* $\boldsymbol{u}$. Therefore, the first-order channel memory within $r_{3(i-1)+1}, r_{3(i-1)+2}, r_{3i}, r_{3i+1}, r_{3i+2}$ is somewhat weakened by the insersion of $r_{3i}$ (due to the transmission of independent $x_{3i}$). Our assumption of blockwisely independence between $r_{3i+1}^{3i+2}$ and $r_{3(i-1)+1}^{3(i-1)+2}$ is thus justified. Simulations confirm that the metrics we obtained based on blockwise independence assumption is only 1-dB away from the Shannon limit. Therefore, it seems reasonable to claim based on our experiments that the first-order channel memory can be nearly compensated by the insertion of one random-bit transmission.

As interleaving operation is applied to the information bit sequence $\boldsymbol{u}$ before it is fed into the second component RSC encoder, the channel memory due to Gauss-Markov fading can be treated as *being neutralized* for the second component decoder. For this reason, the second component decoder assumes its input is interfered with time-independent Gaussian fading channel with $\{h_i\}_{i=1}^N$ being independent Gaussian distributed with the same marginal mean and variance as the Gauss-Markov fading.

## 3.2 Metric functions of the first component MAP decoder

Denote by $t_s^i$ the node at level $i$ with state $s$ over a convolutional code trellis (cf. Fig. 3.1), and let $\mathcal{B}_i^{(u)}$ be the set of trellis edges such that the edge transition from node $t_s^{i-1}$ to node $t_{\bar{s}}^i$ is due to information bit $u_i = u$. For example, there are four nodes at level 4 in Fig. 3.1, which can be respectively represented by $t_0^4$, $t_1^4$, $t_2^4$ and $t_3^4$. In addition, $\mathcal{B}_4^{(0)} = \{(t_0^3, t_0^4), (t_1^3, t_2^4), (t_2^3, t_3^4), (t_3^3, t_1^4)\}$.

As in [1] and [10], the *a posteriori probability* (APP) of $u_i$ upon the reception of $\boldsymbol{d} = [d_1, d_2, \cdots, d_{2K}] = [r_1, r_2, r_4, r_5, \cdots, r_{3K-2}, r_{3K-1}]$ can be represented as:

$$\begin{aligned} \Pr\{u_i = u|\boldsymbol{d}\} &= \sum_{(t_s^{i-1}, t_{\bar{s}}^i) \in \mathcal{B}_i^{(u)}} \Pr\left\{T^{i-1} = t_s^{i-1}, T^i = t_{\bar{s}}^i | \boldsymbol{d}\right\} \\ &= \sum_{(t_s^{i-1}, t_{\bar{s}}^i) \in \mathcal{B}_i^{(u)}} \frac{f\left\{T^{i-1} = t_s^{i-1}, T^i = t_{\bar{s}}^i, \boldsymbol{d}\right\}}{f\{\boldsymbol{d}\}}, \end{aligned} \quad (3.1)$$

where $T^i$ denotes the event of possible visited node at level $i$. For convenience, event $[T^i = t_s^i]$ will be abbreviated as $T_s^i$. Since $T_s^{i-1}$ and $T_{\bar{s}}^i$ considered in $f\{T_s^{i-1}, T_{\bar{s}}^i, \boldsymbol{d}\}$ in (3.1) are required to be in $\mathcal{B}_i^{(u)}$, there must exist a trellis edge inbetween; therefore, it is reasonable to assume that $(T_s^{i-1}, T_{\bar{s}}^i)$-pair in the follow-up derivation can uniquely determine $x_{3(i-1)+1}^{3(i-1)+2}$. We then derive:

$$\begin{aligned} f\left\{T_s^{i-1}, T_{\bar{s}}^i, \boldsymbol{d}\right\} &= f\left\{d_{2i+1}^{2K} \left| T_s^{i-1}, T_{\bar{s}}^i, d_1^{2i}\right.\right\} f\left\{T_s^{i-1}, T_{\bar{s}}^i, d_1^{2i}\right\} \\ &= f\left\{d_{2i+1}^{2K} \left| T_{\bar{s}}^i\right.\right\} f\left\{T_s^{i-1}, d_1^{2(i-1)}\right\} f\left\{T_{\bar{s}}^i, d_{2(i-1)+1}^{2i} \left| T_s^{i-1}, d_1^{2(i-1)}\right.\right\} \\ &= f\left\{d_{2i+1}^{2K} \left| T_{\bar{s}}^i\right.\right\} f\left\{T_s^{i-1}, d_1^{2(i-1)}\right\} f\left\{T_{\bar{s}}^i, d_{2(i-1)+1}^{2i} \left| T_s^{i-1}\right.\right\} \\ &= \beta(T_{\bar{s}}^i)\alpha(T_s^{i-1})\gamma(T_s^{i-1}, T_{\bar{s}}^i), \end{aligned} \quad (3.2)$$

where

$$\alpha(T_s^{i-1}) \triangleq f\left\{T_s^{i-1}, d_1^{2(i-1)}\right\}, \quad \beta(T_{\bar{s}}^i) \triangleq f\left\{d_{2i+1}^{2K} \left| T_{\bar{s}}^i \right.\right\},$$

and

$$\gamma(T_s^{i-1}, T_{\bar{s}}^i) \triangleq f\left\{T_{\bar{s}}^i, d_{2(i-1)+1}^{2i} \left| T_s^{i-1} \right.\right\}.$$

By noting that the number of states of the adopted RSC code is equal to 16, functions $\alpha(\cdot)$ and $\beta(\cdot)$ can be changed into recursive forms through:

$$\begin{aligned}
\alpha(T_s^i) &= f\left\{T_s^i, d_1^{2i}\right\} \\
&= \sum_{\bar{s}=0}^{15} f\left\{T_{\bar{s}}^{i-1}, T_s^i, d_1^{2i}\right\} \\
&= \sum_{\bar{s}=0}^{15} f\left\{T_{\bar{s}}^{i-1}, d_1^{2(i-1)}\right\} f\left\{T_s^i, d_{2(i-1)+1}^{2i} \left| T_{\bar{s}}^{i-1}, d_1^{2(i-1)} \right.\right\} \\
&= \sum_{\bar{s}=0}^{15} f\left\{T_{\bar{s}}^{i-1}, d_1^{2(i-1)}\right\} f\left\{T_s^i, d_{2(i-1)+1}^{2i} \left| T_{\bar{s}}^{i-1} \right.\right\} \\
&= \sum_{\bar{s}=0}^{15} \alpha(T_{\bar{s}}^{i-1})\gamma(T_{\bar{s}}^{i-1}, T_s^i),
\end{aligned}$$

and

$$
\begin{aligned}
\beta(T^i_{\bar{s}}) &= f\left\{ d^{2K}_{2i+1} \middle| T^i_{\bar{s}} \right\} \\
&= \sum_{s=0}^{15} f\left\{ T^{i+1}_s, d^{2K}_{2i+1} \middle| T^i_{\bar{s}} \right\} \\
&= \sum_{s=0}^{15} f\left\{ d^{2K}_{2(i+1)+1} \middle| T^i_{\bar{s}}, T^{i+1}_s, d^{2(i+1)}_{2i+1} \right\} f\left\{ T^{i+1}_s, d^{2(i+1)}_{2i+1} \middle| T^i_{\bar{s}} \right\} \\
&= \sum_{s=0}^{15} f\left\{ d^{2K}_{2(i+1)+1} \middle| T^{i+1}_s \right\} f\left\{ T^{i+1}_s \middle| T^i_{\bar{s}} \right\} \\
&= \sum_{s=0}^{15} \beta(T^{i+1}_s)\gamma(T^i_{\bar{s}}, T^{i+1}_s).
\end{aligned}
$$

We then notice that:

$$
\begin{aligned}
\gamma(T^{i-1}_s, T^i_{\bar{s}}) &= f\left\{ T^i_{\bar{s}}, d^{2i}_{2(i-1)+1} \middle| T^{i-1}_s \right\} \\
&= f\left\{ d^{2i}_{2(i-1)+1} \middle| T^{i-1}_s, T^i_{\bar{s}} \right\} \Pr\left\{ T^i_{\bar{s}} \middle| T^{i-1}_s \right\} \\
&= f\left\{ r^{3(i-1)+2}_{3(i-1)+1} \middle| x^{3(i-1)+2}_{3(i-1)+1} \right\} \Pr\left\{ T^i_{\bar{s}} \middle| T^{i-1}_s \right\}, \qquad (3.3)
\end{aligned}
$$

where $x^{3(i-1)+2}_{3(i-1)+1}$ is the unique codeword portion corresponding to the trellis edge with end nodes $T^{i-1}_s$ and $T^i_{\bar{s}}$. By following similar procedure as in (2.3) (or in [3]), we obtain:

$$
f\left\{ r^{3(i-1)+2}_{3(i-1)+1} \middle| x^{3(i-1)+2}_{3(i-1)+1} \right\} = \frac{e^{-\frac{|\bar{h}_{3(i-1)+1}|^2}{\bar{\sigma}^2_{3(i-1)+1}}}}{\pi^2\sigma^4\sigma_v^2\bar{\sigma}^2_{3(i-1)+1}} \left( \prod_{k=3(i-1)+1}^{3(i-1)+2} e^{-|r_k|^2/\sigma^2} G_k e^{G_k|q_k|^2} \right),
$$

where

$$G_k^{-1} \triangleq \begin{cases} \dfrac{1}{\sigma^2} + \dfrac{|\alpha|^2}{\sigma_v^2} + \dfrac{1}{\bar{\sigma}_k}, & \text{if } k = 3(i-1)+1; \\ \dfrac{1}{\sigma^2} + \dfrac{1}{\sigma_v^2} - \dfrac{|\alpha|^2 G_{k-1}}{\sigma_v^4}, & \text{if } k = 3(i-1)+2, \end{cases}$$

and

$$q_k \triangleq \begin{cases} \dfrac{r_k x_k}{\sigma^2} + \dfrac{\bar{h}_k}{\bar{\sigma}_k^2}, & \text{if } k = 3(i-1)+1; \\ \dfrac{r_k x_k}{\sigma^2} + \dfrac{\alpha G_{k-1} q_{k-1}}{\sigma_v^2}, & \text{if } k = 3(i-1)+2. \end{cases}$$

It remains to consider the last term $\Pr\left\{T_{\bar{s}}^i \middle| T_s^{i-1}\right\}$ in function $\gamma(\cdot)$. Because we always consider those $(T_s^{i-1}, T_{\bar{s}}^i)$-pairs that can define trellis edges,

$$\Pr\left\{T_{\bar{s}}^i \middle| T_s^{i-1}\right\} = \begin{cases} \Pr\{u_i = 0\}, & \text{if } (T_s^{i-1}, T_{\bar{s}}^i) \in \mathcal{B}_i^{(0)}; \\ \Pr\{u_i = 1\}, & \text{if } (T_s^{i-1}, T_{\bar{s}}^i) \in \mathcal{B}_i^{(1)}. \end{cases}$$

Finally, by eliminating product terms that are irrelevant to the choice of $(T_s^{i-1}, T_{\bar{s}}^i)$ (or equivalently, $x_{3(i-1)+1}^{3(i-1)+2}$), we can reduce function $\gamma(\cdot)$ to its equivalent scale without infecting the log-likelihood ratio $\Lambda(i)$ as:

$$\gamma(T_s^{i-1}, T_{\bar{s}}^i) = \begin{cases} \Pr\{u_i = 0\} \displaystyle\prod_{k=1}^{2} e^{G_{3(i-1)+k}\left|q_{3(i-1)+k}\right|^2}, & \text{if } (T_s^{i-1}, T_{\bar{s}}^i) \in \mathcal{B}_i^{(0)}; \\ \Pr\{u_i = 1\} \displaystyle\prod_{k=1}^{2} e^{G_{3(i-1)+k}\left|q_{3(i-1)+k}\right|^2}, & \text{if } (T_s^{i-1}, T_{\bar{s}}^i) \in \mathcal{B}_i^{(1)}; \\ 0, & \text{if } (T_s^{i-1}, T_{\bar{s}}^i) \notin \mathcal{B}_i^{(0)} \cup \mathcal{B}_i^{(1)}, \end{cases} \tag{3.4}$$

where the calculation of $\{|q_{3(i-1)+k}|^2\}_{k=1}^2$ implicitly requires the knowledge of $x_{3(i-1)+1}^{3(i-1)+2}$, which can be determined by $(T_s^{i-1}, T_{\bar{s}}^i)$.

## 3.3 Metric functions of the second component MAP decoder

By assuming that the channel memory has been neutralized by the interleaver, function $\gamma(\cdot)$ for the second component decoder is simplified to:

$$\gamma(T_s^{i-1}, T_{\bar{s}}^{i}) = f\left\{r_{3(\ell(i)-1)+1}\left|x_{3(\ell(i)-1)+1}\right.\right\} f\left\{r_{3i}\left|x_{3i}\right.\right\} \Pr\left\{T_{\bar{s}}^{i}\left|T_s^{i-1}\right.\right\}$$

where $\ell(\cdot)$ denotes the index of interleaved $\boldsymbol{u}$ (namely, $[u_{\ell(1)}, u_{\ell(2)}, \cdots, u_{\ell(K)}]$ is the information input of the second component encoder),

$$f\left\{r_k\left|x_k\right.\right\} = \frac{1}{\pi(\sigma^2+\bar{\sigma}_k^2)} e^{-\frac{|r_k - x_k\bar{h}_k|^2}{\sigma^2+\bar{\sigma}_k^2}} = \frac{e^{-|\bar{h}_k|^2/\bar{\sigma}_k^2}}{\pi\sigma^2\bar{\sigma}_k^2} e^{-|r_k|^2/\sigma^2} \bar{G}_k e^{\bar{G}_k|\bar{q}_k|^2},$$

and

$$\bar{G}_k^{-1} \triangleq \frac{1}{\sigma^2} + \frac{1}{\bar{\sigma}_k^2} \quad \text{and} \quad \bar{q}_k \triangleq \frac{r_k x_k}{\sigma^2} + \frac{\bar{h}_k}{\bar{\sigma}_k^2}.$$

Again, by eliminating product terms that are irrelevant to the choice of $(T_s^{i-1}, T_{\bar{s}}^{i})$, we can reduce function $\gamma(\cdot)$ for the second component decoder to its equivalent scale without infecting the log-likelihood ratio $\Lambda(i)$ as:

$$\gamma(T_s^{i-1}, T_{\bar{s}}^{i}) = \begin{cases} \Pr\left\{u_{\ell(i)} = 0\right\} e^{\bar{G}_{3(\ell(i)-1)+1}|\bar{q}_{3(\ell(i)-1)+1}|^2} e^{\bar{G}_{3i}|\bar{q}_{3i}|^2}, & \text{if } (T_s^{i-1}, T_{\bar{s}}^{i}) \in \mathcal{B}_i^{(0)}; \\ \Pr\left\{u_{\ell(i)} = 1\right\} e^{\bar{G}_{3(\ell(i)-1)+1}|\bar{q}_{3(\ell(i)-1)+1}|^2} e^{\bar{G}_{3i}|\bar{q}_{3i}|^2}, & \text{if } (T_s^{i-1}, T_{\bar{s}}^{i}) \in \mathcal{B}_i^{(1)}; \\ 0, & \text{otherwise.} \end{cases}$$

## 3.4 Iterative MAP decoder

Figure 3.2 illustrates the structure of the iterative MAP decoder. Derive for the first component MAP decoder that:

$$\Lambda_1^{(n)}(i) = \Lambda_{2e}^{(n-1)}(i)+\frac{2G_{3(i-1)+1}}{\sigma^2\bar{\sigma}^2_{3(i-1)+1}}\left(r_{3(i-1)+1}\bar{h}^*_{3(i-1)+1} + r^*_{3(i-1)+1}\bar{h}_{3(i-1)+1}\right)+\Lambda_{1e}^{(n)}(i),$$

where $\Lambda_{2e}^{(n-1)}(i) = \log[\Pr\{u_i = 1\}/\Pr\{u_i = 0\}]$ is the *a priori probability estimate* from the previous stage $(n-1)$, and

$$\Lambda_{1e}^{(n)}(i) \triangleq \log\frac{\sum\limits_{(T_s^{i-1},T_{\bar{s}}^i)\in\mathcal{B}_i^{(1)}}\alpha(T_s^{i-1})\beta(T_{\bar{s}}^i)e^{G_{3(i-1)+2}\left|q_{3(i-1)+2}\right|^2}}{\sum\limits_{(T_s^{i-1},T_{\bar{s}}^i)\in\mathcal{B}_i^{(0)}}\alpha(T_s^{i-1})\beta(T_{\bar{s}}^i)e^{G_{3(i-1)+2}\left|q_{3(i-1)+2}\right|^2}}$$

is the *extrinsic information* that is used to improve the *a priori probability estimate* for the next decoding stage $n$. Similarly, we derive for the second component MAP decoder that:

$$\begin{aligned}\Lambda_2^{(n)}(\ell(i)) &= \Lambda_{1e}^{(n)}(\ell(i)) + \frac{2\bar{G}_{3(\ell(i)-1)+1}}{\sigma^2\bar{\sigma}^2_{3(\ell(i)-1)+1}}\left(r_{3(\ell(i)-1)+1}\bar{h}^*_{3(\ell(i)-1)+1} + r^*_{3(\ell(i)-1)+1}\bar{h}_{3(\ell(i)-1)+1}\right)\\ &\quad +\Lambda_{2e}^{(n)}(\ell(i)),\end{aligned}$$

where

$$\Lambda_{2e}^{(n)}(\ell(i)) \triangleq \log\frac{\sum\limits_{(T_s^{i-1},T_{\bar{s}}^i)\in\mathcal{B}_i^{(1)}}\alpha(T_s^{i-1})\beta(T_{\bar{s}}^i)e^{\bar{G}_{3i}|\bar{q}_{3i}|^2}}{\sum\limits_{(T_s^{i-1},T_{\bar{s}}^i)\in\mathcal{B}_i^{(0)}}\alpha(T_s^{i-1})\beta(T_{\bar{s}}^i)e^{\bar{G}_{3i}|\bar{q}_{3i}|^2}}$$

is the extrinsic information for the second component MAP decoder. The block diagram in Fig. 3.2 then indicates that only the extrinsic information needs to be exchanged between the two component MAP decoders.

We end this chapter by providing the iterative MAP algorithm below for completeness.

**Step 1:** Set $\Lambda_{2e}^{(0)} = 0$, and set $n = 1$.

**Step 2:** Calculate $\mathbf{\Lambda}_1^{(n)}$ and $\mathbf{\Lambda}_{1e}^{(n)}$

1. *Initialization:*

   - For $i = 1, \ldots, K$, $\Pr\{u_i = 0\} = 1/(1 + e^{\Lambda_{2e}^{(n-1)}(i)})$ and $\Pr\{u_i = 1\} = 1 - \Pr\{u_i = 0\}$.

   - For $i = 1, \ldots, K$, $s = 0, \ldots, 15$ and $\bar{s} = 0, \ldots, 15$, compute $\gamma(T_s^{i-1}, T_{\bar{s}}^i)$ as:

$$\gamma(T_s^{i-1}, T_{\bar{s}}^i) = \begin{cases} \Pr\{u_i = 0\} \prod_{k=1}^{2} e^{G_{3(i-1)+k}|q_{3(i-1)+k}|^2}, \text{if } (T_s^{i-1}, T_{\bar{s}}^i) \in \mathcal{B}_i^{(0)}; \\ \Pr\{u_i = 1\} \prod_{k=1}^{2} e^{G_{3(i-1)+k}|q_{3(i-1)+k}|^2}, \text{if } (T_s^{i-1}, T_{\bar{s}}^i) \in \mathcal{B}_i^{(1)}; \\ 0, \quad \text{otherwise.} \end{cases}$$

2. *Forward recursion:*

   - Set $\alpha(T_0^0) = 1$ and for $s = 1, \ldots, 15$, $\alpha(T_s^0) = 0$.

- For $i = 1, \ldots, K$ and $s = 0, \ldots, 15$, perform $\alpha(T_s^i) = \sum_{\bar{s}=0}^{15} \alpha(T_{\bar{s}}^{i-1})\gamma(T_{\bar{s}}^{i-1}, T_s^i)$.

3. *Backward recursion:*

- Set $\beta(T_s^{K+1}) = \alpha(T_s^K)$ for $s = 0, \ldots, 15$.
- For $i = K, \ldots, 1$ and $\bar{s} = 0, \ldots, 15$, perform $\beta(T_{\bar{s}}^i) = \sum_{s=0}^{15} \beta(T_s^{i+1})\gamma(T_{\bar{s}}^i, T_s^{i+1})$.

4. *Soft output:*

- For $i = 1, \ldots, K$, update

$$\Lambda_1^{(n)}(i) = \log \frac{\sum_{(T_s^{i-1}, T_{\bar{s}}^i) \in \mathcal{B}_i^{(1)}} \alpha(T_s^{i-1})\beta(T_{\bar{s}}^i)\gamma(T_s^{i-1}, T_{\bar{s}}^i)}{\sum_{(T_s^{i-1}, T_{\bar{s}}^i) \in \mathcal{B}_i^{(0)}} \alpha(T_s^{i-1})\beta(T_{\bar{s}}^i)\gamma(T_s^{i-1}, T_{\bar{s}}^i)},$$

and

$$\Lambda_{1e}^{(n)}(i) = \Lambda_1^{(n)}(i) - \frac{2G_{3(i-1)+1}}{\sigma^2 \bar{\sigma}_{3(i-1)+1}^2} \left( r_{3(i-1)+1}\bar{h}_{3(i-1)+1}^* + r_{3(i-1)+1}^* \bar{h}_{3(i-1)+1} \right) - \Lambda_{2e}^{(n-1)}(i).$$

**Step 3:** Calculate $\mathbf{\Lambda}_2^{(n)}$ and $\mathbf{\Lambda}_{2e}^{(n)}$.

1. *Initialization:*

- For $i = 1, \ldots, K$, $\Pr\{u_i = 0\} = 1/(1 + e^{\Lambda_{1e}^{(n)}(i)})$ and $\Pr\{u_i = 1\} = 1 - \Pr\{u_i = 0\}$.

- For $i = 1, \ldots, K$, $s = 0, \ldots, 15$ and $\bar{s} = 0, \ldots, 15$, compute $\gamma(T_s^{i-1}, T_{\bar{s}}^i)$ as

$$\gamma(T_s^{i-1}, T_{\bar{s}}^i) = \begin{cases} \Pr\left\{u_{\ell(i)} = 0\right\} e^{\bar{G}_{3(\ell(i)-1)+1}|\bar{q}_{3(\ell(i)-1)+1}|^2} e^{\bar{G}_{3i}|\bar{q}_{3i}|^2}, \text{if } (T_s^{i-1}, T_{\bar{s}}^i) \in \mathcal{B}_i^{(0)}; \\ \Pr\left\{u_{\ell(i)} = 1\right\} e^{\bar{G}_{3(\ell(i)-1)+1}|\bar{q}_{3(\ell(i)-1)+1}|^2} e^{\bar{G}_{3i}|\bar{q}_{3i}|^2}, \text{if } (T_s^{i-1}, T_{\bar{s}}^i) \in \mathcal{B}_i^{(1)}; \\ 0, \qquad \text{if } (T_s^{i-1}, T_{\bar{s}}^i) \notin \mathcal{B}_i^{(0)} \cup \mathcal{B}_i^{(1)}. \end{cases}$$

2. *Forward recursion:*

   - Set $\alpha(T_0^0) = 1$ and for $s = 1, \ldots, 15$, $\alpha(T_s^0) = 0$.
   - For $i = 1, \ldots, K$ and $s = 0, \ldots, 15$, perform $\alpha(T_s^i) = \sum_{\bar{s}=0}^{15} \alpha(T_{\bar{s}}^{i-1})\gamma(T_{\bar{s}}^{i-1}, T_s^i)$.

3. *Backward recursion:*

   - Set $\beta(T_s^{K+1}) = \alpha(T_s^K)$ for $s = 0, \ldots, 15$.
   - For $i = K, \ldots, 1$ and $\bar{s} = 0, \ldots, 15$, perform $\beta(T_{\bar{s}}^i) = \sum_{s=0}^{15} \beta(T_s^{i+1})\gamma(T_{\bar{s}}^i, T_s^{i+1})$.

4. *Soft output:*

   - For $i = 1, \ldots, K$, update

$$\Lambda_2^{(n)}(\ell(i)) = \log \frac{\sum_{(T_s^{i-1}, T_{\bar{s}}^i) \in \mathcal{B}_i^{(1)}} \alpha(T_s^{i-1})\beta(T_{\bar{s}}^i)\gamma(T_s^{i-1}, T_{\bar{s}}^i)}{\sum_{(T_s^{i-1}, T_{\bar{s}}^i) \in \mathcal{B}_i^{(0)}} \alpha(T_s^{i-1})\beta(T_{\bar{s}}^i)\gamma(T_s^{i-1}, T_{\bar{s}}^i)},$$

and

$$\begin{aligned}\Lambda_{2e}^{(n)}(\ell(i)) &= \Lambda_{2}^{(n)}(\ell(i)) - \Lambda_{1e}^{(n)}(\ell(i)) \\ &\quad - \frac{2\bar{G}_{3(\ell(i)-1)+1}}{\sigma^2\bar{\sigma}^2_{3(\ell(i)-1)+1}}\left(r_{3(\ell(i)-1)+1}\bar{h}^*_{3(\ell(i)-1)+1} + r^*_{3(\ell(i)-1)+1}\bar{h}_{3(\ell(i)-1)+1}\right).\end{aligned}$$

**Step 4:** Repeat Step 2 and Step 3 (by setting $n = n + 1$) until the number of desired iterations is reached, and make final hard-decision based on the last $\mathbf{\Lambda_2}$.

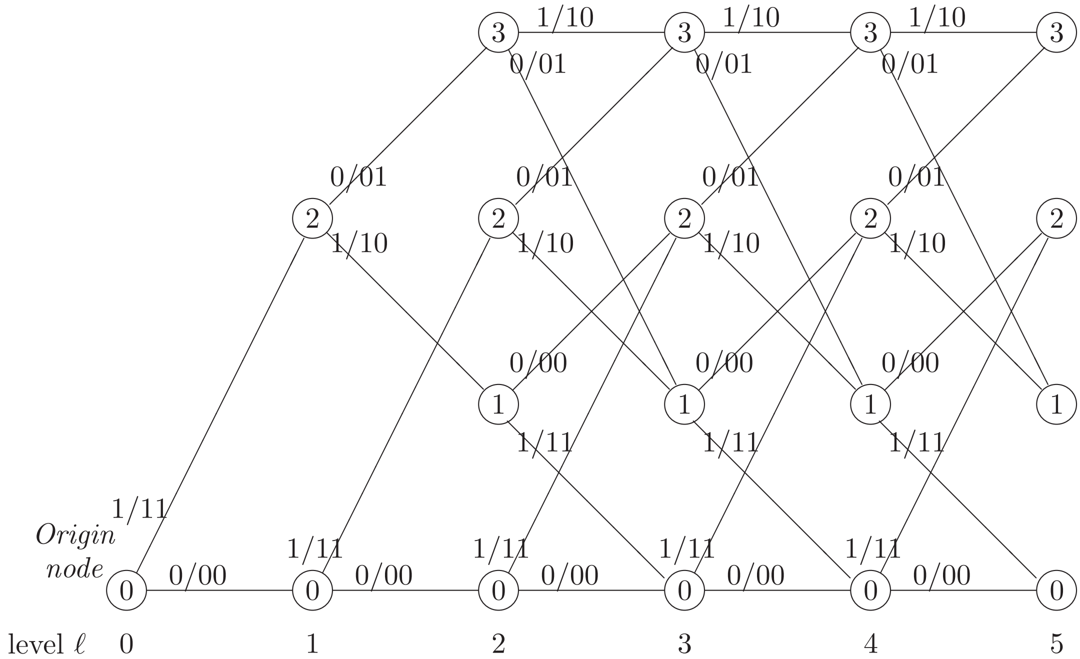


Figure 3.1: Trellis diagram for a $(7, 5)$ RSC code with memory order 2. The numbers inside circles indicate the states of the nodes at the specific level. The information bit and the two code bits along with a trellis edge are marked above the edge.

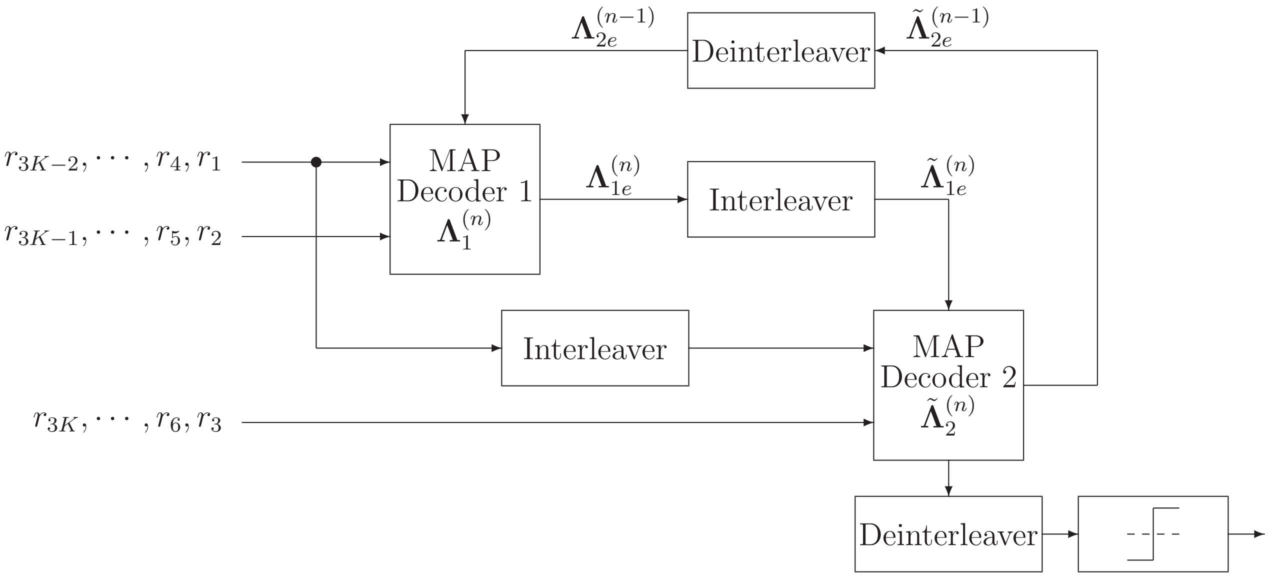


Figure 3.2: Block diagram of the iterative MAP decoder. A tilde over the vector represents its interleaved version.

# Chapter 4

# Simulation Results for Iterative MAP Decoder

## 4.1 System setting and channel parameters

In our simulations, the Berrou-Glavieux interleaver with size $256 \times 256$ is employed [2, 7]. Thus, $K = 65536$ and $N = 3 \times 65536$. Similar to [3], we take $\alpha = 0.995$, $h_0 = (0.5 \text{ or } 1)$ and $\sigma_v^2 = (0.001 \text{ or } 0.01)$. Furthermore, the channel fading is reset every 99 symbols; as a result, $\bar{h}_i = \alpha^{[(i-1) \bmod 99]+1} h_0$ and $\bar{\sigma}_i^2 = \sigma_v^2 \frac{(1-|\alpha|^{2([(i-1) \bmod 99]+1)})}{(1-|\alpha|^2)}$.[1]

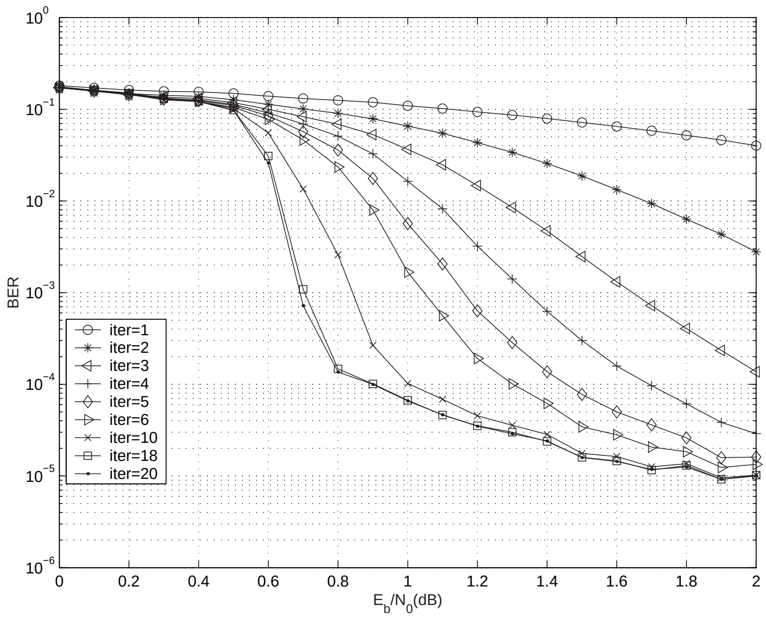


Figure 4.1: Performance curve of the proposed iterative MAP decoder. Parameters of Gauss-Markov channel are $\alpha = 0.995$, $\sigma_v^2 = 0.001$ and $h_0 = 1$.

## 4.2 Simulation Results

Figure 4.1 shows the performance of the proposed iterative MAP decoder for channel parameters $h_0 = 1$ and $\sigma_v^2 = 0.001$. It indicates that the bit-error-rate (BER) decreases as the number of iterations increases from 1 to 20. Since the BER performance for 20 iterations is very close to that for 18 iterations, it is reasonable to anticipate that no further improvement can be obtained with more iterations. Besides, error floor can be observed in this figure. The performance curve for 20 iterations has apparently lower slope when $E_b/N_0$ is beyond 0.8 dB.

Figure 4.2 depicts the difference between the performance of the iterative MAP algorithm and a lower bound of the Shannon limit (cf. Appendix A.1). The figure shows that when $\sigma_v^2 = 0.001$ and $h_0 = 1$, the resultant performance curve of the iterative MAP algorithm is only 0.9 dB

[1] In our figures, the computation of $E_b/N_0$ follows the formula below.

$$\begin{aligned} E_b/N_0 &= \frac{\overline{\text{SNR}}}{R} = \frac{1}{R} \times \frac{\sum_{k=1}^{N} E[|h_k|^2]}{N\sigma^2} = \frac{1}{R} \times \frac{\sum_{k=1}^{N} |\bar{h}_k|^2 + \sum_{k=1}^{N} \bar{\sigma}_k^2}{N\sigma^2} \\ &= \frac{1}{R} \times \frac{|h_0|^2 \sum_{k=1}^{N} |\alpha|^{2[(k-1) \bmod 99+1]} + \frac{\sigma_v^2}{1-|\alpha|^2} \sum_{k=1}^{N} (1 - |\alpha|^{2[(k-1) \bmod 99+1]})}{N\sigma^2} \\ &= \frac{1}{R} \left( \frac{|h_0|^2}{\sigma^2} \cdot \frac{|\alpha|^2(1-|\alpha|^{198})}{99(1-|\alpha|^2)} + \frac{\sigma_v^2}{\sigma^2} \cdot \frac{99 - 100|\alpha|^2 + |\alpha|^{200}}{99(1-|\alpha|^2)^2} \right) \end{aligned}$$

where $R$ is the channel code rate, and $N$ is assumed to be a multiple of 99 for convenience.

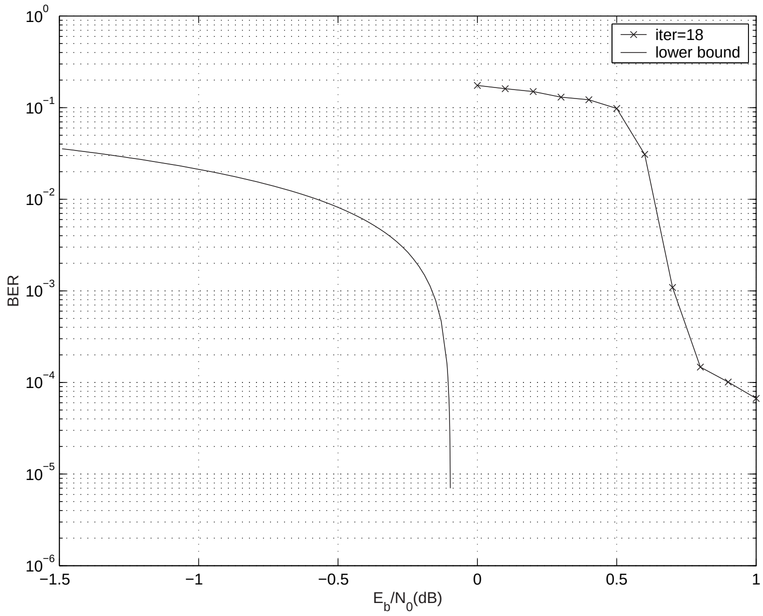


Figure 4.2: Performance comparison between the iterative MAP decoder with 18 iterations and a lower bound (cf. Appendix I) of the Shannon limit. Parameters of Gauss-Markov channel are $\alpha = 0.995$, $\sigma_v^2 = 0.001$ and $h_0 = 1$.

away from the lower bound at BER $= 2 \times 10^{-4}$. Therefore, the iterative MAP algorithm is at most 0.9 dB away from the true Shannon limit at BER $= 2 \times 10^{-4}$.

Figures 4.3 and 4.4 display how iterations improve the decoding performance when channel parameters are respectively $\{h_0 = 0.5,\ \sigma_v^2 = 0.001\}$ and $\{h_0 = 1,\ \sigma_v^2 = 0.01\}$. Notably, a smaller $h_0$ or a larger $\sigma_v^2$ in concept give a *noisier* channel. Unlike the previous channel setting, the performances in the two figures saturate with much less iterations. When $h_0 = 0.5$ and $\sigma_v^2 = 0.001$, the iterative MAP algorithm with 13 iterations performs close to that with 20 iterations. When $h_0 = 1$ and $\sigma_v^2 = 0.01$, the sufficient number of iterations, which saturates the performance, reduces to seven.

From Figs. 4.1, 4.3 and 4.4, the performance of the iterative MAP decoder degrades as $h_0$ decreases or $\sigma_v^2$ increases as anticipated. For parameters $h_0 = 0.5$ and $\sigma_v^2 = 0.001$, the BER reaches $2 \times 10^{-4}$ when $E_b/N_0 = 3.2$ dB. For Gauss-Markov channel defined by $h_0 = 1$ and $\sigma_v^2 = 0.01$, the iterative MAP decoder requires $E_b/N_0 = 8$ dB to obtain the same BER. In fact, we observe that the performance of the iterative MAP decoder is more sensitive to the variation of $\sigma_v^2$ than that of $h_0$.

It is worth mentioning that the proposed iterative MAP algorithm only

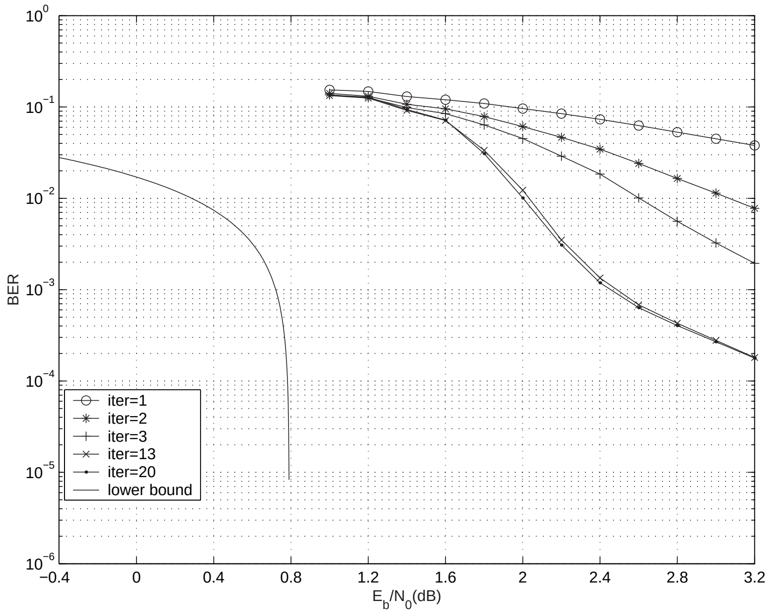


Figure 4.3: Performance comparison between the iterative MAP decoding and a lower bound of the Shannon limit. Parameters of Gauss-Markov channel are $\alpha = 0.995$, $\sigma_v^2 = 0.001$ and $h_0 = 0.5$.

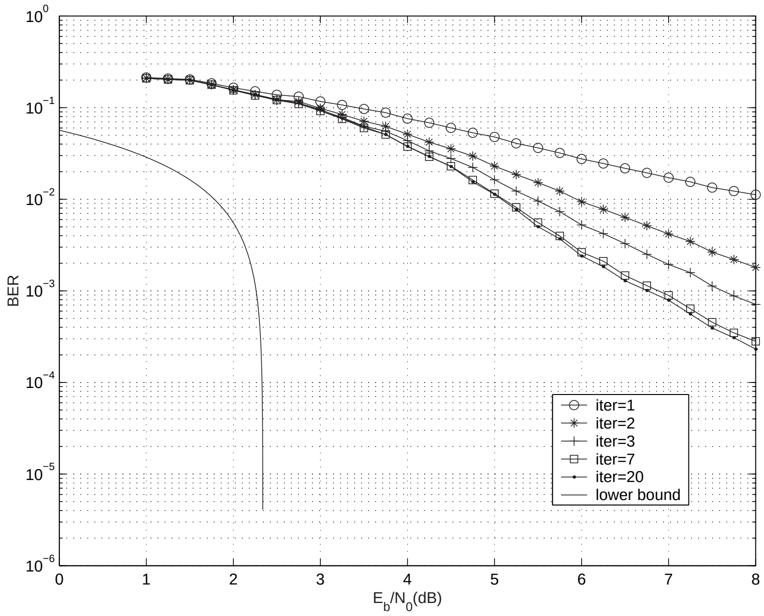


Figure 4.4: Performance comparison between the iterative MAP decoding and a lower bound of the Shannon limit. Parameters of Gauss-Markov channel are $\alpha = 0.995$, $\sigma_v^2 = 0.01$ and $h_0 = 1$.

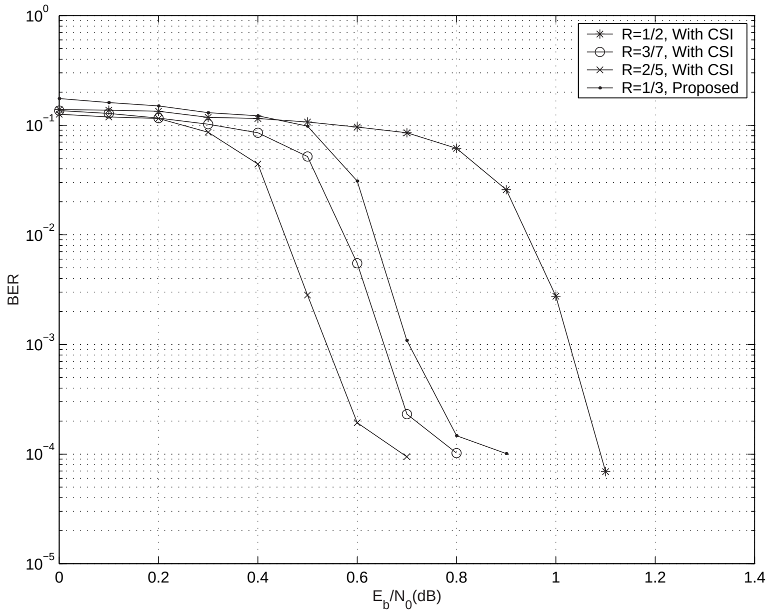


Figure 4.5: Performances of punctured PCCC codes with code rates 1/2, 3/7 and 2/5. The CSIs are assumed known for the iterative MAP decoder of these punctured code. For comparison, the performance of the proposed blind-CSI iterative MAP algorithm is also depicted. All of them are decoded with 18 iterations. Parameters of Gauss-Markov channel are $\alpha = 0.995$, $\sigma_v^2 = 0.001$ and $h_0 = 1$.

requires the knowledge of channel statistics, and does not presume the existence of the channel estimation circuitry at the receiver. Thus, the system we considered does not need to transmit, e.g., training sequence for the estimation of channel states. In Fig. 4.5, we simulated three kinds of punctured PCCC codes with code rates 1/2, 3/7 and 2/5 under channel parameters $h_0 = 1$ and $\sigma_v^2 = 0.001$. Since these code rates are all higher than 1/3, we assume that the remaining transmitted bits (i.e., $N/3$, $2N/9$ and $N/6$ bits respectively for 1/2, 3/7 and 2/5 punctured codes) can be used as training bits to establish *perfect* channel estimation of $\boldsymbol{h} = [h_1, h_2, \cdots, h_N]$. The iterative MAP decoder, in such case, reduces to the conventional one derived for AWGN channels. The simulation results show that only rate-2/5 and rate-3/7 punctured systems with perfect channel state information (CSI) perform better than the proposed blind-CSI iterative MAP algorithm, but the performance deviations are limited respectively within 0.2 and 0.1 dB at BER $= 10^{-4}$. Since it is in general hard to achieve accurate channel estimation for a time-varying channel even with a large number of training bits, the small performance derivation merits the usage of the proposed blind-CSI iterative MAP algorithm.

# Chapter 5

# Conclusion and Future Work

In this work, we take the PCCC code and its respective iterative MAP decoder as a test vehicle to experiment on the idea that the *temporal channel memory* can be weakened to *nearly blockwise time-independence* by the insertive transmission of informationless “random bits” of sufficient length between two consecutive blocks, for which these “random bits” are actually another parity check bits generated due to interleaved information bits. The simulation results show that the metrics derived based on blockwise independence with 2-bit blocks periodically separated by *single* parity-check bit from the second component RSC encoder perform close to the CSI-aided decoding scheme, and is at most 0.9 dB away from the Shannon limit at BER $= 2 \times 10^{-4}$ when $h_0 = 1$ and $\sigma_v^2 = 0.001$. A natural future work is to extend the channel memory to higher order, and further examine whether the same idea can be applied to obtain well-acceptable system performance.

# Appendix A

## Supplemental Derivations

### A.1 A lower bound of the Shannon limit

The capacity of the simulated Gauss-Markov channel is given by: $C \triangleq \frac{1}{99}\max_{x^{99}} I\left(x^{99}; r^{99}\right)$, where $x^{99} \in \{-1,+1\}^{99}$ and $r^{99}$ are respectively the channel input and output of the Gauss-Markov channel, and $I(\cdot;\cdot)$ represents the mutual information function. Then,

$$C \leq \frac{1}{99}\max_{x^{99}}\sum_{k=1}^{99} I(x_k; r_k) \leq \frac{1}{99}\sum_{k=1}^{99}\max_{x_k} I(x_k; r_k) = \frac{1}{99}\sum_{k=1}^{99}\max_{x_k}\left[h(r_k) - h(r_k|x_k)\right],$$

where $h(\cdot)$ is the differential entropy function. Observe that

$$\begin{aligned}
h(r_k|x_k) &= \sum_{x_k\in\{-1,+1\}} \Pr\{x_k\}\int_{\mathcal{C}} f\{r_k|x_k\}\log\frac{1}{f\{r_k|x_k\}}dr_k \\
&= \sum_{X_k}\Pr\{x_k\}\int_{\mathcal{C}}\frac{1}{\pi(\sigma^2+\bar{\sigma}_k^2)}e^{-\frac{|r_k-x_k\bar{h}_k|^2}{\sigma^2+\bar{\sigma}_k^2}}\left(\log\left[\pi(\sigma^2+\bar{\sigma}_k^2)\right]+\frac{|r_k-x_k\bar{h}_k|^2}{\sigma^2+\bar{\sigma}_k^2}\right)dr_k \\
&= \sum_{X_k}\Pr\{x_k\}\cdot\log\left[\pi e\left(\sigma^2+\bar{\sigma}_k^2\right)\right] = \log\left[\pi e\left(\sigma^2+\bar{\sigma}_k^2\right)\right]
\end{aligned}$$

is independent of $x_k$. Hence, $\max_{x_k} I(x_k; r_k) = \max_{x_k} h(r_k) - \log\left[\pi e\left(\sigma^2 + \bar{\sigma}_k^2\right)\right]$.

Since $h(r_k)$ is maximized by $\Pr\{x_k = +1\} = \Pr\{x_k = -1\} = 1/2$,

$$\begin{aligned}
\max_{x_k} h(r_k) &= \int_{\mathcal{C}} \frac{1}{2\pi(\sigma^2+\bar{\sigma}_k^2)} \left( e^{-\frac{|r_k-\bar{h}_k|^2}{\sigma^2+\bar{\sigma}_k^2}} + e^{-\frac{|r_k+\bar{h}_k|^2}{\sigma^2+\bar{\sigma}_k^2}} \right) \\
&\quad \left[ \log\left(2\pi(\sigma^2+\bar{\sigma}_k^2)\right) + \frac{|r_k|^2+|\bar{h}_k|^2}{\sigma^2+\bar{\sigma}_k^2} - \log\left( e^{\frac{r_k\bar{h}_k^*+r_k^*\bar{h}_k}{\sigma^2+\bar{\sigma}_k^2}} + e^{-\frac{r_k\bar{h}_k^*+r_k^*\bar{h}_k}{\sigma^2+\bar{\sigma}_k^2}} \right) \right] dr_k \\
&= \log\left(2\pi e(\sigma^2+\bar{\sigma}_k^2)\right) + 2\frac{|\bar{h}_k|^2}{\sigma^2+\bar{\sigma}_k^2} - \int_{\mathcal{C}} \frac{1}{\pi(\sigma^2+\bar{\sigma}_k^2)} e^{-\frac{|r_k-\bar{h}_k|^2}{\sigma^2+\bar{\sigma}_k^2}} \log(2) dr_k \\
&\quad - \int_{\mathcal{C}} \frac{1}{\pi(\sigma^2+\bar{\sigma}_k^2)} e^{-\frac{|r_k-\bar{h}_k|^2}{\sigma^2+\bar{\sigma}_k^2}} \log\left( \frac{e^{\frac{r_k\bar{h}_k^*+r_k^*\bar{h}_k}{\sigma^2+\bar{\sigma}_k^2}} + e^{-\frac{r_k\bar{h}_k^*+r_k^*\bar{h}_k}{\sigma^2+\bar{\sigma}_k^2}}}{2} \right) dr_k \\
&= \log\left(\pi e(\sigma^2+\bar{\sigma}_k^2)\right) + \frac{2|\bar{h}_k|^2}{\sigma^2+\bar{\sigma}_k^2} \\
&\quad - \frac{\sqrt{\sigma^2+\bar{\sigma}_k^2}}{|\bar{h}_k|\sqrt{\pi}} \int_{\Re} e^{-\frac{(\sigma^2+\bar{\sigma}_k^2)}{|\bar{h}_k|^2}\left(t-\frac{|\bar{h}_k|^2}{\sigma^2+\bar{\sigma}_k^2}\right)^2} \log\left(\cosh(2t)\right) dt,
\end{aligned}$$

where the last step follows by letting $t = \frac{r_k\bar{h}_k^*+r_k^*\bar{h}_k}{2(\sigma^2+\bar{\sigma}_k^2)}$ and $s = \frac{r_k\bar{h}_k^*-r_k^*\bar{h}_k}{2j(\sigma^2+\bar{\sigma}_k^2)}$, applying Jacobian transformation [8, pp. 227-229] to real-valued $t$ and $s$, and taking integration with respect to $s$. As a result,

$$\begin{aligned}
C &\leq C_{\mathrm{UP}} \\
&\triangleq \frac{1}{99}\sum_{k=1}^{99} \left[ |\rho_k|^2 - \frac{1}{\sqrt{2\pi}} \int_{\Re} e^{-v^2/2} \log\left(\cosh\left(|\rho_k| v + |\rho_k|^2\right)\right) dv \right],
\end{aligned}$$

where $v = \frac{2}{|\rho_k|}\left(t - \frac{|\rho_k|^2}{2}\right)$ and $\rho_k \triangleq \sqrt{2}\cdot\bar{h}_k/\sqrt{\sigma^2+\bar{\sigma}_k^2}$. By joint source-channel coding theorem [6, pp. 215-218], the Shannon limit can be defined by the equation:

$$\log(2) - H_b(\mathrm{BER}) = \frac{C}{R},$$

where the left-hand-side is the rate-distortion function for a binary input and Hamming additive distortion measure, and $H_b(t) = -t \cdot \log t - (1-t) \cdot \log(1-t)$ is the binary entropy function. Combining all the above derivations, we obtain: $H_b(\mathrm{BER}) \geq \log(2) - C_{\mathrm{UP}}/R$.

## A.2 Detail derivation for Eq. (2.3)

$$\begin{aligned}
f\left\{r_i^j | x_i^j\right\} &= \int_{\mathcal{C}^{j-i+1}} \left( \frac{1}{(\pi\sigma^2)^{j-i+1}} \prod_{k=i}^{j} e^{-\frac{|r_k - x_k h_k|^2}{\sigma^2}} \right) \left( \frac{1}{(\pi\sigma_v^2)^{j-i}(\pi\bar{\sigma}_i^2)} e^{-\frac{|h_i - \bar{h}_i|^2}{\bar{\sigma}_i^2}} \right. \\
&\qquad \left. \prod_{k=i+1}^{j} e^{-\frac{|h_k - \alpha h_{k-1}|^2}{\sigma_v^2}} \right) dh_i^j \\
&= \frac{1}{\pi^{2(j-i+1)}\sigma^{2(j-i+1)}\sigma_v^{2(j-i)}\bar{\sigma}_i^2} \int_{\mathcal{C}^{j-i}} \left( \prod_{k=i+1}^{j} e^{-\frac{|r_k - x_k h_k|^2}{\sigma^2}} \right) \left( \prod_{k=i+2}^{j} e^{-\frac{|h_k - \alpha h_{k-1}|^2}{\sigma_v^2}} \right) \\
&\qquad \left( \int_{\mathcal{C}} e^{-\frac{|r_i - x_i h_i|^2}{\sigma^2} - \frac{|h_i - \bar{h}_i|^2}{\bar{\sigma}_i^2} - \frac{|h_{i+1} - \alpha h_i|^2}{\sigma_v^2}} dh_i \right) dh_{i+1}^j. \qquad \text{(A.1)}
\end{aligned}$$

Since $x_i$ is either $+1$ or $-1$, the exponent in the inner integral can be re-written as:

$$
\begin{aligned}
& \frac{|r_i - x_i h_i|^2}{\sigma^2} + \frac{|h_i - \bar{h}_i|^2}{\bar{\sigma}_i^2} + \frac{|h_{i+1} - \alpha h_i|^2}{\sigma_v^2} \\
= \; & \frac{1}{\sigma^2}\left(|r_i|^2 - r_i x_i h_i^* - r_i^* x_i h_i + |h_i|^2\right) + \frac{1}{\bar{\sigma}_i^2}\left(|h_i|^2 - h_i \bar{h}_i^* - h_i^* \bar{h}_i + |\bar{h}_i|^2\right) \\
& + \frac{1}{\sigma_v^2}\left(|h_{i+1}|^2 - \alpha^* h_{i+1} h_i^* - \alpha h_{i+1}^* h_i + |\alpha|^2 |h_i|^2\right) \\
= \; & |h_i|^2 \left(\frac{1}{\sigma^2} + \frac{1}{\bar{\sigma}_i^2} + \frac{|\alpha|^2}{\sigma_v^2}\right) - h_i \left(\frac{r_i^* x_i}{\sigma^2} + \frac{\bar{h}_i^*}{\bar{\sigma}_i^2} + \frac{\alpha h_{i+1}^*}{\sigma_v^2}\right) \\
& - h_i^* \left(\frac{r_i x_i}{\sigma^2} + \frac{\bar{h}_i}{\bar{\sigma}_i^2} + \frac{\alpha^* h_{i+1}}{\sigma_v^2}\right) + \left(\frac{|r_i|^2}{\sigma^2} + \frac{|\bar{h}_i|^2}{\bar{\sigma}_i^2} + \frac{|h_{i+1}|^2}{\sigma_v^2}\right) \\
= \; & |h_i|^2 G_i^{-1} - h_i g_i^* G_i^{-1} - h_i^* g_i G_i^{-1} + \left(\frac{|r_i|^2}{\sigma^2} + \frac{|\bar{h}_i|^2}{\bar{\sigma}_i^2} + \frac{|h_{i+1}|^2}{\sigma_v^2}\right) \\
= \; & |h_i - g_i|^2 G_i^{-1} - |g_i|^2 G_i^{-1} + \left(\frac{|r_i|^2}{\sigma^2} + \frac{|\bar{h}_i|^2}{\bar{\sigma}_i^2} + \frac{|h_{i+1}|^2}{\sigma_v^2}\right),
\end{aligned}
$$

where

$$
g_i \triangleq G_i \left(q_i + \frac{\alpha^* h_{i+1}}{\sigma_v^2}\right), \quad G_i^{-1} \triangleq \frac{1}{\sigma^2} + \frac{|\alpha|^2}{\sigma_v^2} + \frac{1}{\bar{\sigma}_i^2}, \quad \text{and} \quad q_i \triangleq \frac{r_i x_i}{\sigma^2} + \frac{\bar{h}_i}{\bar{\sigma}_i^2}.
$$

Since

$$
\int_{\mathcal{C}} e^{-|h_i - g_i|^2 G_i^{-1}} dh_i = \pi G_i,
$$

the exponent terms remained after the integration of the inner integral are given by:

$$
\begin{aligned}
& -|g_i|^2 G_i^{-1} + \left( \frac{|r_i|^2}{\sigma^2} + \frac{|\bar{h}_i|^2}{\bar{\sigma}_i^2} + \frac{|h_{i+1}|^2}{\sigma_v^2} \right) \\
= \; & -\left| G_i \left( q_i + \frac{\alpha^* h_{i+1}}{\sigma_v^2} \right) \right|^2 G_i^{-1} + \left( \frac{|r_i|^2}{\sigma^2} + \frac{|\bar{h}_i|^2}{\bar{\sigma}_i^2} + \frac{|h_{i+1}|^2}{\sigma_v^2} \right) \\
= \; & -G_i \left( |q_i|^2 + q_i \frac{\alpha h_{i+1}^*}{\sigma_v^2} + q_i^* \frac{\alpha^* h_{i+1}}{\sigma_v^2} + \frac{|\alpha|^2 |h_{i+1}|^2}{\sigma_v^4} \right) \\
& + \left( \frac{|r_i|^2}{\sigma^2} + \frac{|\bar{h}_i|^2}{\bar{\sigma}_i^2} + \frac{|h_{i+1}|^2}{\sigma_v^2} \right) \\
= \; & \frac{\sigma_v^2 - |\alpha|^2 G_i}{\sigma_v^4} |h_{i+1}|^2 - \frac{\alpha q_i G_i}{\sigma_v^2} h_{i+1}^* - \frac{\alpha^* q_i^* G_i}{\sigma_v^2} h_{i+1} - G_i |q_i|^2 + \frac{|r_i|^2}{\sigma^2} + \frac{|\bar{h}_i|^2}{\bar{\sigma}_i^2} \\
= \; & \frac{|h_{i+1} - \bar{h}_{i+1}|^2}{\bar{\sigma}_{i+1}^2} - G_i |q_i|^2 - \frac{|\bar{h}_{i+1}|^2}{\bar{\sigma}_{i+1}^2} + \frac{|r_i|^2}{\sigma^2} + \frac{|\bar{h}_i|^2}{\bar{\sigma}_i^2},
\end{aligned}
$$

where

$$
\frac{1}{\bar{\sigma}_{i+1}^2} \triangleq \frac{\sigma_v^2 - |\alpha|^2 G_i}{\sigma_v^4} = \frac{\frac{\sigma_v^2}{\sigma^2} + \frac{\sigma_v^2}{\bar{\sigma}_i^2}}{\sigma_v^4 \left[ \frac{1}{\sigma^2} + \frac{|\alpha|^2}{\sigma_v^2} + \frac{1}{\bar{\sigma}_i^2} \right]} > 0 \quad \text{and} \quad \bar{h}_{i+1} \triangleq \frac{\alpha q_i G_i \bar{\sigma}_{i+1}^2}{\sigma_v^2}.
$$

Consequently,

$$
\begin{aligned}
f\left\{ r_i^j | x_i^j \right\} = \; & \frac{e^{|\bar{h}_{i+1}|^2/\bar{\sigma}_{i+1}^2 - |\bar{h}_i|^2/\bar{\sigma}_i^2}}{\pi^{2(j-i)+1} \sigma^{2(j-i+1)} \sigma_v^{2(j-i)} \bar{\sigma}_i^2} e^{-|r_i|^2/\sigma^2} G_i e^{G_i |q_i|^2} \\
& \int_{\mathcal{C}^{j-i-1}} \left( \prod_{k=i+2}^{j} e^{-\frac{|r_k - x_k h_k|^2}{\sigma^2}} \right) \left( \prod_{k=i+3}^{j} e^{-\frac{|h_k - \alpha h_{k-1}|^2}{\sigma_v^2}} \right) \\
& \left( \int_{\mathcal{C}} e^{-\frac{|r_{i+1} - x_{i+1} h_{i+1}|^2}{\sigma^2} - \frac{|h_{i+1} - \bar{h}_{i+1}|^2}{\bar{\sigma}_{i+1}^2} - \frac{|h_{i+2} - \alpha h_{i+1}|^2}{\sigma_v^2}} dh_{i+1} \right) dh_{i+2}^j .
\end{aligned}
\tag{A.2}
$$

Similarly, the exponent in the inner integral in (A.2) can be re-written as:

$$\begin{aligned}
&\frac{|r_{i+1}-x_{i+1}h_{i+1}|^2}{\sigma^2}+\frac{|h_{i+1}-\bar{h}_{i+1}|^2}{\bar{\sigma}_{i+1}^2}+\frac{|h_{i+2}-\alpha h_{i+1}|^2}{\sigma_v^2} \\
= \; &|h_{i+1}-g_{i+1}|^2 G_{i+1}^{-1}-|g_{i+1}|^2 G_{i+1}^{-1}+\left(\frac{|r_{i+1}|^2}{\sigma^2}+\frac{|\bar{h}_{i+1}|^2}{\bar{\sigma}_{i+1}^2}+\frac{|h_{i+2}|^2}{\sigma_v^2}\right),
\end{aligned}$$

where

$$g_{i+1} \triangleq G_{i+1}\left(q_{i+1}+\frac{\alpha^* h_{i+2}}{\sigma_v^2}\right),$$

$$G_{i+1}^{-1} \triangleq \frac{1}{\sigma^2}+\frac{|\alpha|^2}{\sigma_v^2}+\frac{1}{\bar{\sigma}_{i+1}^2}=\frac{1}{\sigma^2}+\frac{|\alpha|^2}{\sigma_v^2}+\frac{1}{\sigma_v^2}-\frac{|\alpha|^2 G_i}{\sigma_v^4}$$

and

$$q_{i+1} \triangleq \frac{r_{i+1}x_{i+1}}{\sigma^2}+\frac{\bar{h}_{i+1}}{\bar{\sigma}_{i+1}^2}=\frac{r_{i+1}x_{i+1}}{\sigma^2}+\frac{\alpha q_i G_i}{\sigma_v^2}.$$

Hence,

$$\begin{aligned}
f\left\{r_i^j|x_i^j\right\} = \; &\frac{1}{\pi^{2(j-i)}\sigma^{2(j-i+1)}\sigma_v^{2(j-i)}\bar{\sigma}_i^2}\left(\prod_{k=i}^{i+1} e^{|\bar{h}_{k+1}|^2/\bar{\sigma}_{k+1}^2-|\bar{h}_k|^2/\bar{\sigma}_k^2}\cdot e^{-|r_k|^2/\sigma^2}\cdot G_k e^{G_k|q_k|^2}\right) \\
&\int_{\mathcal{C}^{j-i-2}}\left(\prod_{k=i+3}^{j} e^{-\frac{|r_k-x_k h_k|^2}{\sigma^2}}\right)\left(\prod_{k=i+4}^{j} e^{-\frac{|h_k-\alpha h_{k-1}|^2}{\sigma_v^2}}\right) \\
&\left(\int_{\mathcal{C}} e^{-\frac{|r_{i+2}-x_{i+2}h_{i+2}|^2}{\sigma^2}-\frac{|h_{i+2}-\bar{h}_{i+2}|^2}{\bar{\sigma}_{i+2}^2}-\frac{|h_{i+3}-\alpha h_{i+2}|^2}{\sigma_v^2}} dh_{i+2}\right) dh_{i+3}^j.
\end{aligned}$$

Continue the above procedure until we obtain:

$$\begin{aligned}
f\left\{r_i^j|x_i^j\right\} = \; &\frac{1}{\pi^{j-i+1}\sigma^{2(j-i+1)}\sigma_v^{2(j-i)}\bar{\sigma}_i^2}\left(\prod_{k=i}^{j-1} e^{|\bar{h}_{k+1}|^2/\bar{\sigma}_{k+1}^2-|\bar{h}_k|^2/\bar{\sigma}_k^2}\cdot e^{-|r_k|^2/\sigma^2}\cdot G_k e^{G_k|q_k|^2}\right) \\
&\int_{\mathcal{C}} e^{-\frac{|r_j-x_j h_j|^2}{\sigma^2}-\frac{|h_j-\bar{h}_j|^2}{\bar{\sigma}_j^2}} dh_j. \qquad (A.3)
\end{aligned}$$

The exponent in the integral in (A.3) equals:

$$
\begin{aligned}
& \frac{|r_j - x_j h_j|^2}{\sigma^2} + \frac{|h_j - \bar{h}_j|^2}{\bar{\sigma}_j^2} \\
= \; & \frac{1}{\sigma^2}\left(|r_j|^2 - r_j x_j h_j^* - r_j^* x_j h_j + |h_j|^2\right) + \frac{1}{\bar{\sigma}_j^2}\left(|h_j|^2 - h_j \bar{h}_j^* - h_j^* \bar{h}_j + |\bar{h}_j|^2\right) \\
= \; & |h_j|^2 \left(\frac{1}{\sigma^2} + \frac{1}{\bar{\sigma}_j^2}\right) - h_j \left(\frac{r_j^* x_j}{\sigma^2} + \frac{\bar{h}_j^*}{\bar{\sigma}_j^2}\right) - h_j^* \left(\frac{r_j x_j}{\sigma^2} + \frac{\bar{h}_j}{\bar{\sigma}_j^2}\right) + \left(\frac{|r_j|^2}{\sigma^2} + \frac{|\bar{h}_j|^2}{\bar{\sigma}_j^2}\right) \\
= \; & |h_j|^2 G_j^{-1} - h_j g_j^* G_j^{-1} - h_j^* g_j G_j^{-1} + \left(\frac{|r_j|^2}{\sigma^2} + \frac{|\bar{h}_j|^2}{\bar{\sigma}_j^2}\right) \\
= \; & |h_j - g_j|^2 G_j^{-1} - |g_j|^2 G_j^{-1} + \left(\frac{|r_j|^2}{\sigma^2} + \frac{|\bar{h}_j|^2}{\bar{\sigma}_j^2}\right),
\end{aligned}
$$

where

$$
g_j \triangleq q_j G_j, \quad G_j^{-1} \triangleq \frac{1}{\sigma^2} + \frac{1}{\bar{\sigma}_j^2} = \frac{1}{\sigma^2} + \frac{1}{\sigma_v^2} - \frac{|\alpha|^2 G_{j-1}}{\sigma_v^4}
$$

and

$$
q_j \triangleq \frac{r_j x_j}{\sigma^2} + \frac{\bar{h}_j}{\bar{\sigma}_j^2} = \frac{r_j x_j}{\sigma^2} + \frac{\alpha q_{j-1} G_{j-1}}{\sigma_v^2}.
$$

Since

$$
\begin{aligned}
-|g_j|^2 G_j^{-1} + \left(\frac{|r_j|^2}{\sigma^2} + \frac{|\bar{h}_j|^2}{\bar{\sigma}_j^2}\right) &= -\left|G_j q_j\right|^2 G_j^{-1} + \left(\frac{|r_j|^2}{\sigma^2} + \frac{|\bar{h}_j|^2}{\bar{\sigma}_j^2}\right) \\
&= -G_j |q_j|^2 + \frac{|r_j|^2}{\sigma^2} + \frac{|\bar{h}_j|^2}{\bar{\sigma}_j^2},
\end{aligned}
$$

the final expression for $f\left\{r_i^j | x_i^j\right\}$ is established as:

$$
f\left\{r_i^j | x_i^j\right\} = \frac{e^{-|\bar{h}_i|^2/\bar{\sigma}_i^2}}{\pi^{j-i+1}\sigma^{2(j-i+1)}\sigma_v^{2(j-i)}\bar{\sigma}_i^2} \left(\prod_{k=i}^{j} e^{-|r_k|^2/\sigma^2} G_k e^{G_k |q_k|^2}\right).
$$

## A.3 Berrou-Glavieux interleaver

The Berrou-Glavieux interleaver [2,7] fetches data into an $M \times M$ matrix in a row-by-row manner, and then reads out according to a nonuniform rule as $\ell(M \times i + j) = M \times \bar{i} + \bar{j}$, where

$$\bar{i} = \left(\frac{M}{2} + 1\right)(i + j) \mod M, \text{ and } \bar{j} = ([P((i + j) \mod 8) \cdot (j + 1)] - 1) \mod M,$$

and $P(0) = 17, P(1) = 37, P(2) = 19, P(3) = 29, P(4) = 41, P(5) = 23, P(6) = 13, P(7) = 7.$

BIBLIOGRAPHY

[1] L. R. Bahl, J. Cocke, F. Jelinek and J. Raviv, "Optimal decoding of linear codes for minimizing symbol error rate," *IEEE Trans. Inform. Theory*, vol. 20, no. 2, pp. 284-287, March 1974.

[2] C. Berrou and A. Glavieux, "Near optimum error correcting coding and decoding: Turbo-codes," *IEEE Trans. Commun.*, vol. 44, no. 10, pp. 1261-1271, October 1996.

[3] H. Chen, K. Buckley and R. Perry, "Time-recursive maximum likelihood based sequence estimation for unknown ISI channels," in *Proc. 34th Asilomar Conf. Signals, Systems, Computers*, vol. 2, pp. 1005-1009, November 2000.

[4] H. Chen, R. Perry, and K. Buckley, "On MLSE algorithms for unknown fast time-varying channels" *IEEE Trans. Commun.*, vol. 51 , no. 5 , pp. 730-734, May 2003.

[5] IEEE Std 802.11a-1999, *Part 11: Wireless LAN Medium Access Control (MAC) and Physical Layer (PHY) Specications: High-speed Physical Layer In The 5 GHz Band*, September 1999.

[6] T. M. Cover and Joy A. Thomas, *Elements of Information Theory* John Wiley & Sons, 1991.

[7] C. Heegard and S. B. Wicker, *Turbo Coding*, Kluwer Academic Publishers, 1999.

[8] A. Leon-Garcia, *Probability and Random Processes for Electrical Engineering*, Addison-Wesley Publishing Company, 1994.

[9] M. Stojanovic and Z. Zvonar, "Performance of multiuser diversity reception in Rayleigh fading CDMA channels," *IEEE Trans. Commun.*, vol. 47, no. 3, pp. 356-359, March 1999.

[10] B. Vucetic and J. Yuan, *Turbo codes: Principles and Applications*, Kluwer Academic Publishers, 2000.